frontiers | Frontiers in Energy Research

TYPE Original Research
PUBLISHED 27 March 2024
DOI 10.3389/fenrg.2024.1370412

OPEN ACCESS

EDITED BY
Enrico Maria Vitucci,
University of Bologna, Italy

REVIEWED BY
Dheeraj Joshi,
Delhi Technological University, India
Nishant Kumar,
Indian Institute of Technology Jodhpur, India

*CORRESPONDENCE
Shitharath Selvarajan,
s.selvarajan@leedsbeckett.ac.uk

RECEIVED 14 January 2024
ACCEPTED 13 March 2024
PUBLISHED 27 March 2024

CITATION
Srilakshmi K, Sundaragiri D, Gaddameedhi S, Vangalapudi R, Balachandran PK, Colak I and Selvarajan S (2024), Simulation of grid/standalone solar energy supplied reduced switch converter with optimal fuzzy logic controller using golden BallAlgorithm. *Front. Energy Res.* 12:1370412. doi: 10.3389/fenrg.2024.1370412

Simulation of grid/standalone solar energy supplied reduced switch converter with optimal fuzzy logic controller using golden BallAlgorithm

Koganti Srilakshmi[1], Dheeraj Sundaragiri[2], Sravanthy Gaddameedhi[1], Ramprasad Vangalapudi[1], Praveen Kumar Balachandran[3], Ilhami Colak[4] and Shitharath Selvarajan[5]*

[1]Department of Electrical and Electronics Engineering, Sreenidhi Institute of Science and Technology, Hyderabad, Telangana, India, [2]Department of Computer Science and Engineering, Sreenidhi Institute of Science and Technology, Hyderabad, Telangana, India, [3]Department of Electrical and Electronics Engineering, Vardhaman College of Engineering, Hyderabad, Telangana, India, [4]Department of Electrical and Electronics Engineering, Faculty of Engineering and Architectures, Nisantasi University, Istanbul, Türkiye, [5]Cyber Security and Digital Forensics, School of Built Environment, Engineering and Computing, Leeds Beckett University, Leeds, United Kingdom

This article presents the utilization of a shunt active power filter (SHAPF) in combination with an Energy Storage System (ESS) and a Solar Energy System (SES). Voltage source converters (VSC) are connected in parallel to a direct current (DC) bus. The membership function (MSF) of fuzzy logic controller (FLC) for the shunt control system is optimally adjusted using the golden balloptimization algorithm (GBOA). The present effort aims to achieve the following primary objectives: 1) Quick implementation to stabilize the voltage of the DC Link capacitor (DCLCV); 2) Mitigation of harmonics and improvement of power factor (PF); 3) Satisfactory performance under load as well as solar power varying conditions. The effectiveness of the optimally designed controller is evaluated by studying four test scenarios with grid and standalone conditions. The results are then compared to the existing sliding mode (SMC) and fuzzy logic controllers (FLC).

KEYWORDS

fuzzy logic controller, golden ball optimization algorithm, solar system, battery system, reduced switch converter

1 Introduction

Promoting the insertion of sources of clean energy, such as wind and solar energy, into the network of distribution has been encouraged over the past few years to reduce the burden on converters and ratings. The word "reduced switch" refers to achieving its objectives with a reduced number of switches in comparison to conventional systems. This reduction in the number of switches can lead to benefits such as lower cost, reduced power losses, and improved reliability. Like other active power filters, reduced Switch Shunt Active Power Filters play a crucial role in maintaining a stable and high-quality electrical power

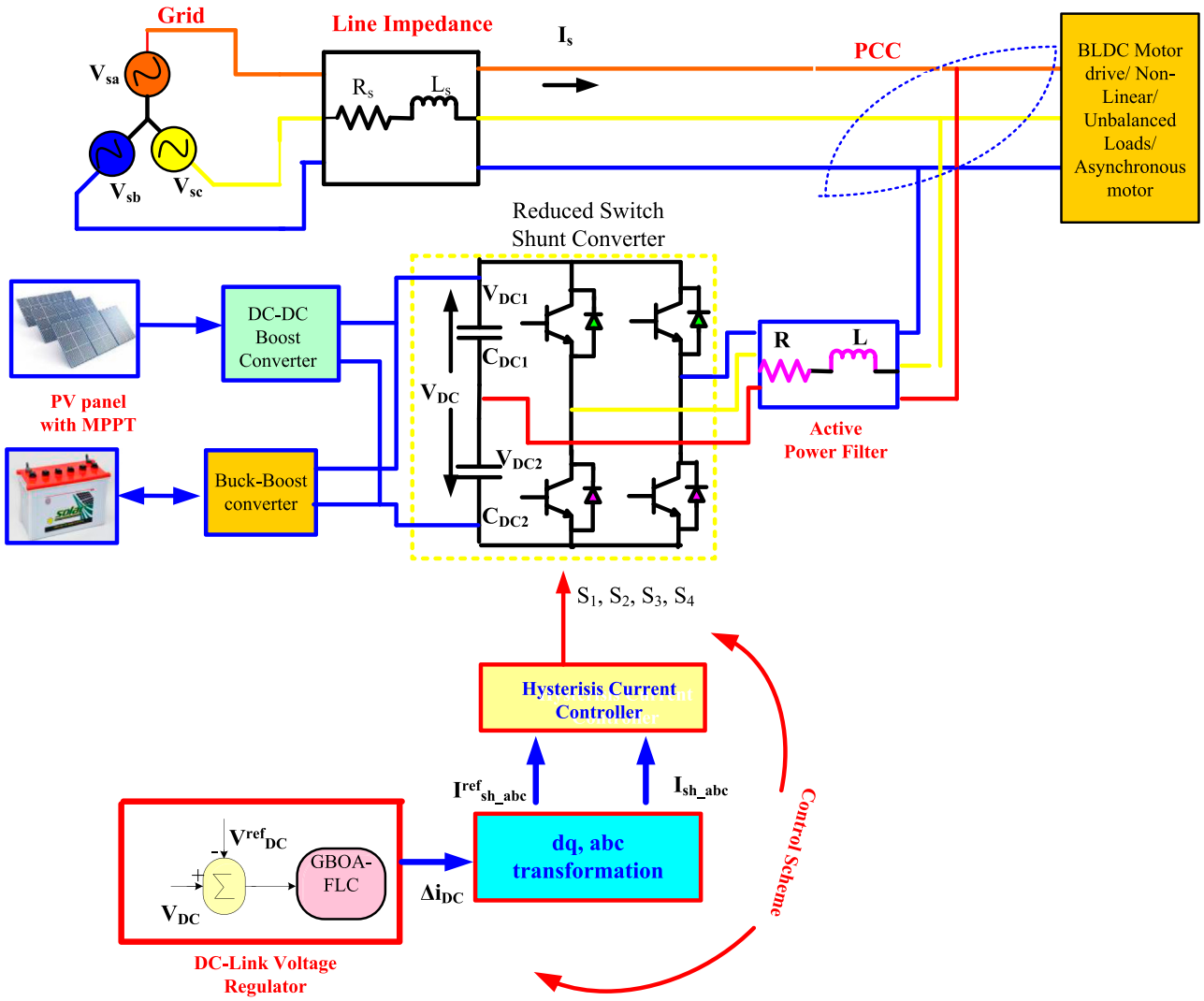

FIGURE 1
Reduced switch VSC.

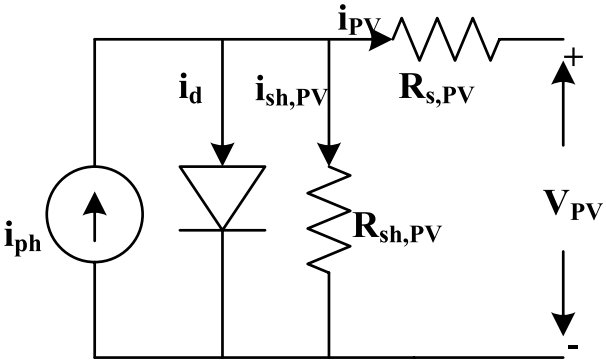

FIGURE 2
PV single-cell model.

supply in modern power systems. Their design and operation may vary based on specific requirements and the characteristics of the power system.

1.1 Motivation

The significance of SHAPF in distributed power generation systems and micro-grids has lately garnered attention. The integration of SHAPF with alternative sources of energy has become increasingly important compared to the traditional grid-connected VSC. This strategy has several benefits, including the capacity to keep a steady (DCLCV) despite load swings enhance Power Quality (PQ) on the grid, safeguard sensitive equipment from disturbances originating from the grid, and enhance the converter's ability to withstand transient events. Besides, the 3-phase, 3-wire distribution networks are particularly suitable for utilizing shunt filters with clean energy sources. Most of the techniques described in current literature papers are with conventional proportional integral controller (PIC), SMC, and artificial intelligence (AI) methods involving various loads. However, these methods have not successfully obtained optimized values during change in irradiation and load.

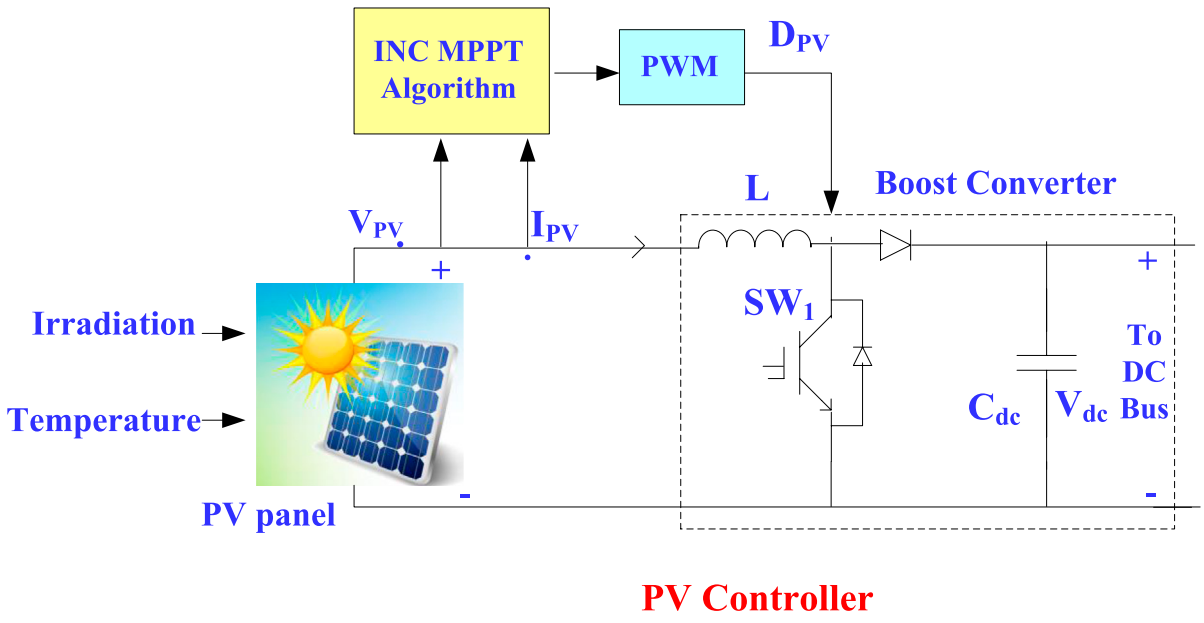

FIGURE 3
Control of SES system.

1.2 Literature survey

A novel automated transition mechanism has been devised for the SES and ESS tie UPQC to address PQ challenges in grid and island modes effectively. Moreover, the system's function was validated using empirical data (Devassy and Singh, 2020). An evaluation was undertaken to assess the performance of the SES and ESS for UPQC utilizing the Adaptive Neuro-Fuzzy Inference System (ANFIS) technique. This system was designed to improve PQ. The evaluation was conducted under different demand and supply instances (Dheeban and MuthuSelvan, 2021). In addition, it was proposed to combine UPQC with PV systems using an adaptive compensation technique. This technique utilizes the variable leaky least mean square (VLLMS) algorithm to eliminate the need for a low-pass or moving average filter. Instead, it extracts the fundamental components from the distorting input voltage and load current. It generates a reference signal to regulate the VSCS switching operations in the UPQC (Ray et al., 2022). Simultaneously, a computational challenge was presented to identify the optimal positions and setups for grid-connected PV systems. The purpose is to enhance the reliability of power generation by maximizing the efficiency of PV systems in diverse scenarios with varying generation probabilities (Tawfiq et al., 2021).

The adaptive distributed power control technique was proposed to address problems such as THD and voltage aberrations. This technique involves using two H-connected arrangements, each consisting of eight switches, for the 3-ω UPQC (Mohanraj and Prakash, 2020). Additionally, the PPDM was implemented for the UPQC in the context of a multilayer Cascaded Inverter. The principal objective is to reduce fluctuation in voltage (sag and swell), manage harmonics, and maintain a stable DCLCV (Vinothkumar and Kanimozhi, 2021). A performance comparison was conducted between the P & O and PSO algorithms to get maximum power point tracking system (MPPT) for the PV system during changes in irradiance. The micro-inverter adjusts to partial circumstances (Jaber and Shakir, 2021a). Furthermore, a multi-level cascade UPQC was developed to mitigate voltage supply abnormalities and THD by utilizing PV, wind, and Proton Exchange Membrane Fuel Cells (PEMFCS) as power sources (Sarker et al., 2020).

The UPQC system, associated with ESS and SES, was suggested to mitigate THD and resolve grid voltage problems (AlifMansor et al., 2020). Besides, the study investigated several control techniques and algorithms for UPQC to improve PQ. As a result, a flexible control strategy was recommended (SaiSarita et al., 2021). The SES-supplied Synchronous Uninterruptible Active Power Filter was developed to control reactive power effectively and minimize THD in current waveforms. However, to generate appropriate reference currents, the Maxikalman filter was designed (Das et al., 2021). Meanwhile, ANN controller, utilizing feed-forward training, was implemented in a UPQC system connected to SES and WES sources. This controller was used for voltage regulation and control of reactive power inside the grid (Chandrasekaran et al., 2021).

The UPQC was employed to correct voltage imbalances, reduce current harmonics imperfections, and improve network efficiency. This was accomplished by incorporating an adaptive ANFIS controller (Renduchintala et al., 2021). The FLC was suggested for incorporating the series filter into the grid-tie three-phase distribution system to tackle power quality issues such as voltage fluctuations, decreased total harmonic distortion of the current signal, and continuous maintenance of DCLCV stability (Pazhanimuthu and Ramesh, 2018). However, a specialized SRFT technique utilizing a PIC was designed specifically for the synchronous uninterruptible SHAPF connected with the fuel cell. The main goal is to decrease the existing harmonics with DCLCV

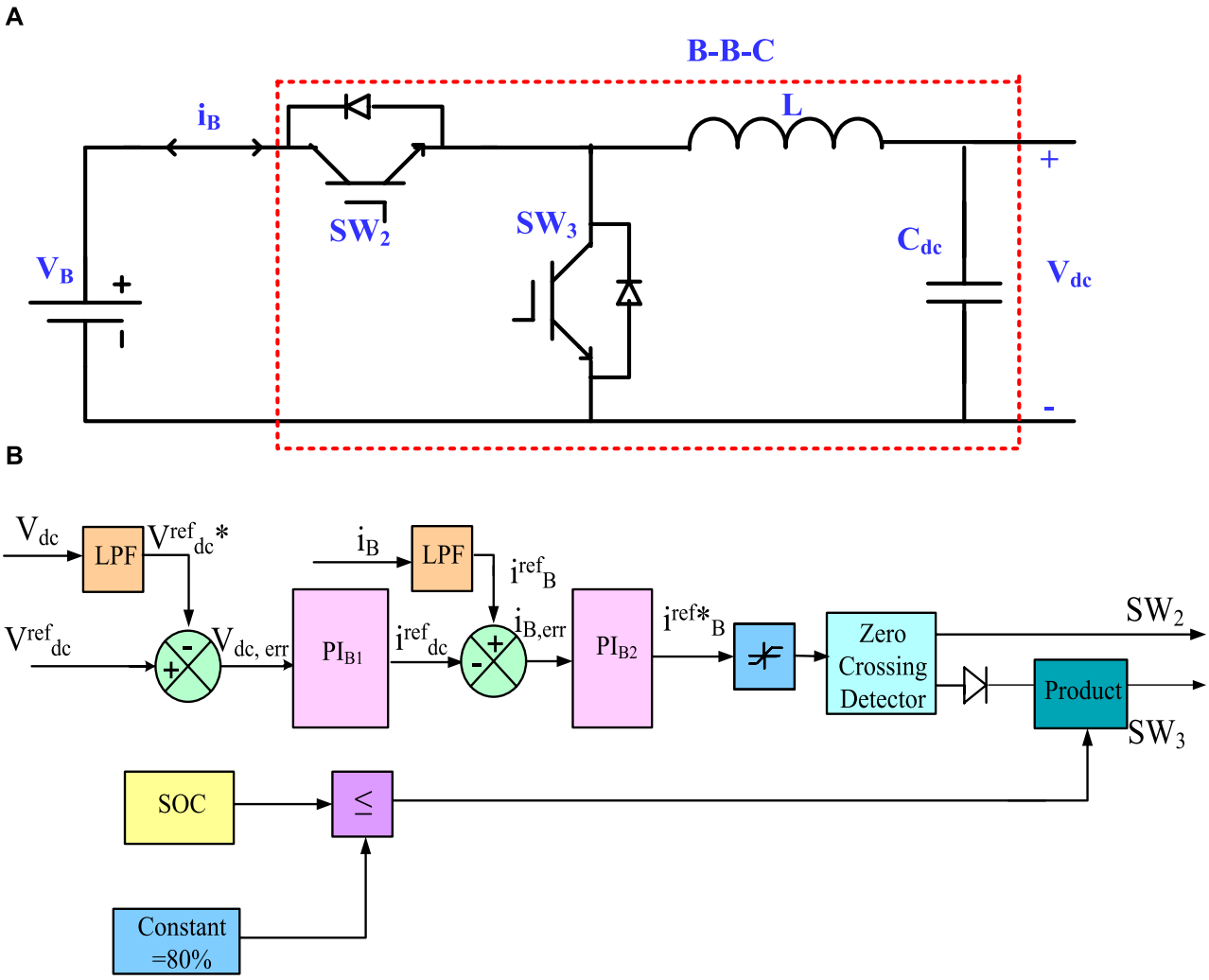

FIGURE 4
ESS. **(A)** ESS configuration at DC link **(B)** ESS controller.

TABLE 1 Power dispersion at DC link.

Modes of operation	Action taken
Mode-1: When No SES	Only ESS will supply power to P_L
Mode-2: When SES = P_L	Solar PV supply power to P_L
Mode-3: When SES< P_L	The battery will supply the cumulative difference in power until till $SOCB_{min}$
Mode-4: When SES> P_L	The surplus solar electricity is utilized to charge the Battery system until it reaches $SOCB_{max}$

stable (K Krishna et al., 2020). The idea entailed the integration of intelligent Fuzzy-PI and Fuzzy-PID controllers into an AC-DC micro-grid to address PQ issues and enhance voltage stability. Moreover, the effectiveness of the controllers was demonstrated through two scenarios involving different levels of loads (Abdelnasser et al., 2022).

An adaptive full-order technique is proposed to improve UPQC by reliably detecting faults in dynamic load variations and grid circumstances. In addition, a BBO metaheuristic technique was utilized to tune the gain parameters of the PIC to stabilize DCLCV oscillations (Sayed et al., 2021) efficiently. On other hand, the experimental setup of a full bridge DC-DC converter was examined along with a snubber circuit (Jaber and Shakir, 2021a). A novel hybrid control approach was developed by integrating the Improved Bat Algorithm and Moth Flame Algorithm to tackle power quality concerns in a micro-grid system effectively. The objective of this strategy is to reduce the error function that is linked to power variations. Fine-tuning the Kp and Ki parameters optimally can minimize the operational expenses associated with renewable energy sources (Rajesh et al., 2021). A

TABLE 2 SES and ESS ratings.

Equipment	Factor	Value chosen
PV single panel (Sun power SPR-305E-WHT-D)	PV cells connected in parallel, series	66, 5
	Maximum PV Output power	305.22W
	Under max power the current/voltage	5.58A/54.7V
	Voltage under open circuit condition	64.2V
	Current under short circuit condition	5.96A
Li-ion battery	Fully charge voltage	350V
	Rated Capacity of battery	35Ah

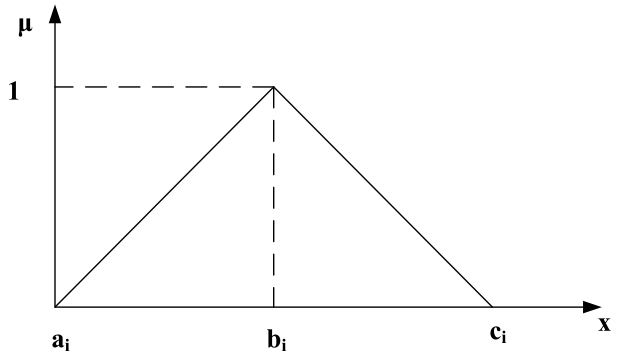

FIGURE 5
Triangular MSF.

hybrid control system incorporating fuzzy back-propagation was used to a 5-level UPQC to decrease THD and improve the power factor (Nagireddy et al., 2018). In addition, a unique method was proposed to combine sequence-component identification with unit vector-template creation for the double-stage SES UPQC. This method aims to address PQ problems (Nkado et al., 2021).

A novel control method utilizing a damped fifth-order generalized integrator was proposed for grid-integrated solar photovoltaic (PV) systems. Furthermore, the GMPPT utilizes the HPO algorithm. A grid-integrated partially shaded PV array with a single-stage topology, consisting of three phases and three wires, was built. The HPO algorithm exhibits speedy and accurate global maximum power peak seeking behaviour, resulting in good steady-state and dynamic performances, even under rapid solar irradiance change (Kumar et al., 2019). On the other hand, a technology called adaptive Maximize-M Kalman filter is utilized for better optimal control. In order to optimize the amount of power extracted from a solar PV panel, a grid-integrated solar PV system utilizes a learning-based hill-climbing algorithm (Kumar et al., 2020).

However, a model predictive control algorithm is used to manage and control the power transmission between a solar PV system and the grid efficiently. The double stage three-phase design is regulated utilizing a model predictive control technique that considers the power converters' switching states to anticipate the next control variable. The control utilizes a modified-dual second-order generalized-integrator to estimate the power demands, taking into account the continuously changing system parameters (Saxena et al., 2021). Meanwhile, a novel voltage sensorless model predictive control approach was proposed for efficient and rapid maximum power extraction from a PV array in a solar-powered on-board electric vehicle (EV) charging system. The VSPC system employs the initial model predictive control technique, utilizing a PV array to forecast the system's condition within a specific time frame and to eliminate the need for a voltage sensor (Kumar et al., 2023).

Besides, a novel command authentication strategy was developed to detect and mitigate false data injection attacks targeting the system centralized economic dispatch control signals (Siu et al., 2022). A revolutionary hill climbing MPPT algorithm was created using a parabolic curve fitting to efficiently harvest the maximum power from solar PV panels. This algorithm was designed for residential customers and can adapt to changing environmental circumstances. Furthermore, the advanced PCHC algorithm has been combined with an innovative decreased sensor-based method, in which a solitary current sensor is employed to charge the solar-powered battery (Kumari et al., 2023).

However, the hybrid fuzzy-sliding mode control (HFSMC) based maximum-power-point tracking system (MPPTs) is adopted for solar PV system to extract maximum output (Srilakshmi et al., 2023). Besides, the design of Unified Power Quality Conditioner (UPQC) through the optimal selection of the active filter and PID Controller parameters using the enhanced most valuable player algorithm (EMVPA) was suggested to handle PQ issues (SrilakshmiKoganti et al., 2024). Besides, the soccer league algorithm-based optimal tuned hybrid controller for the UPQC was designed for PQ enhancement (Srilakshmi et al., 2022). On the other hand, the optimal training of neural network controller was proposed for the UPQC to handle PQ problems (AlapatiRamadevi et al., 2023). The Optimal design of artificial neuro fuzzy controller member ship function was carried out with the firefly and harmony search algorithms (Srilakshmi et al., 2024).

1.3 Key contribution

The following steps emphasize the contribution of this manuscript:

- Introducing the SHAPF using the nature-inspired metaheuristic GBOA.

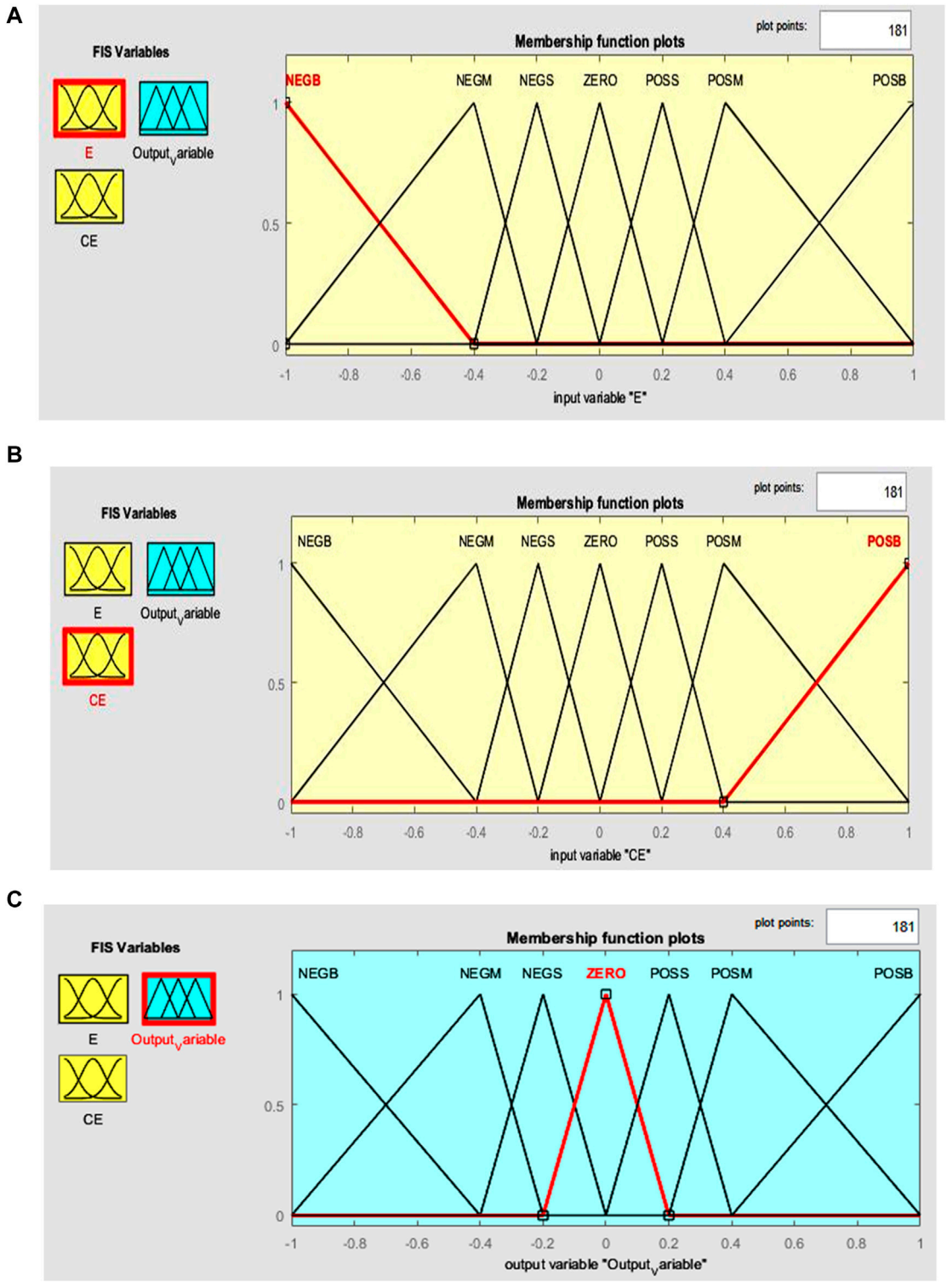

FIGURE 6
Optimal MSF with GBOA. **(A)** E **(B)** CE **(C)** Output.

- Design of reduced switch SHAPF.
- Optimal selection of MSF parameters for reduced switch SHAPFwith GBOA in order to minimize imperfections in the current waveforms and appropriate power supply to the load.
- Integrating the SES and ESS into the DC connection of the proposed reduced switch VSC reduces the burden and stress on the filter. This integration will also enable the filter to fulfill load demands and maintain a steady DCLCV even during changes in demand and irradiation.

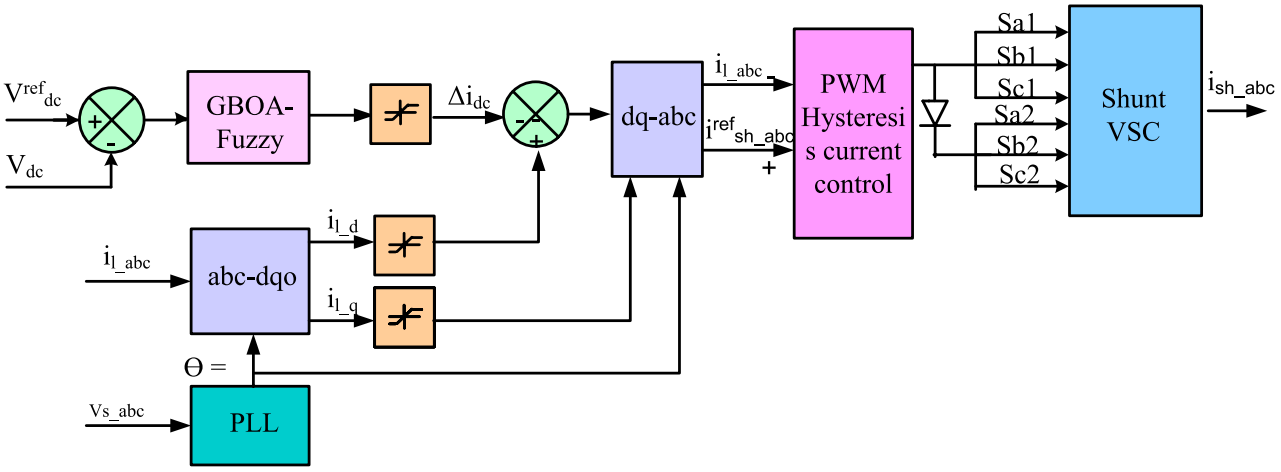

FIGURE 7
Hybrid controller for shunt converter.

➢ The proposed strategy is to enhance power factor, achieve consistent direct current line current variation within a brief timeframe, and minimize total harmonic distortion of the source current. To further show the efficiency of the suggested approach, it is subjected to examination under four different situations, each characterized by changing loads and Sun irradiation levels as well as grid and standalone conditions.

The structure of this paper is as outlined below: Section 2 covers the reduced switch VSC, focusing on its external sources. Section 3 describes the recommended control system with GBOA. Section 4 gives the outcomes and discussions. Finally, Section 5 ends the manuscript.

2 System design and modeling

Figure 1 depicts the block diagram of the SHAPF connected to the DC link, along with ESS and SES. When coupled in parallel to the load, the inverter acts as SHAPF to compensate the harmonics in the load current while simultaneously maintaining DCLCV. In the conventional inverter configuration, a more significant number of switches are needed. This work utilizes a simplified switch configuration for an inverter of a SHAPF. The Modified low Switch SHAPF technique decreases the number of switches in the Bridged VSC from six to four. Split capacitors are used to connect the third phase. Figure 1 depicts the proposed VSC, with various load types.

2.1 Design of SHAPF

The fundamental role of SHAPF is to provide a distortion-free supply current by injecting the required amount of current at the point of common coupling (PCC). The control circuit uses Eqs 1–4, to calculate the necessary magnitude of compensated current.

$$i_s = i_l - i_{sh} \tag{1}$$

$$V_s = V_m \sin wt \tag{2}$$

$$i_l = \sum_{n=1}^{\infty} i_n \sin(nwt + \varphi_n) = i_1 \sin(wt + \varphi_1) + \sum_{n=1}^{\infty} i_n \sin(nwt + \varphi_n) \tag{3}$$

$$P_L = V_s{}^{*} i_l \tag{4}$$

Where, “Vm” denotes the amplitude voltage of the sinusoidal signal, “n” resembles the nth harmonic current, “il” indicates load current, “ish” gives the shunt filter compensating current, PLis the load power, Eq 5 can be utilized to obtain the numerical value of Cdc

$$C_{dc} = \frac{\pi^{*} i_{sh}}{\sqrt{3}\omega V_{cr,pp}} \tag{5}$$

The V_{dc}^{ref} selection is made from the available ratings provided by the proposed method. The choice is determined by the peak-to-peak voltage ripple ($V_{cr,pp}$) and the shunt adjusting current. The inductor (Lsh) links the shunt VSC to the network and its characteristics are determined by the DCLCV, switching frequency, and ripple current as mentioned in Eq. 6:

$$L_{sh,\min} = \frac{\sqrt{3}\, m\, V_{dc}}{12\, a_f\, f_{sh}\, I_{cr,pp}} \tag{6}$$

The value of (L_{sh}) is determined by the switching frequency (f_{sh}) is 10 kHz, the peak-to-peak ripples ($I_{cr,pp}$), the overloading factor (a_f) is 1.5with the assumption that the modulation depth (m) is 1.

2.2 Mathematical modelling of the external sources and modes of operation

The reduced switch VSC is recommended for employing the SES and ESS to supply the DC link. The DCLCV is regulated by a sustainable energy source with the support of ESS assistance during fluctuations in power demand. These external sources of

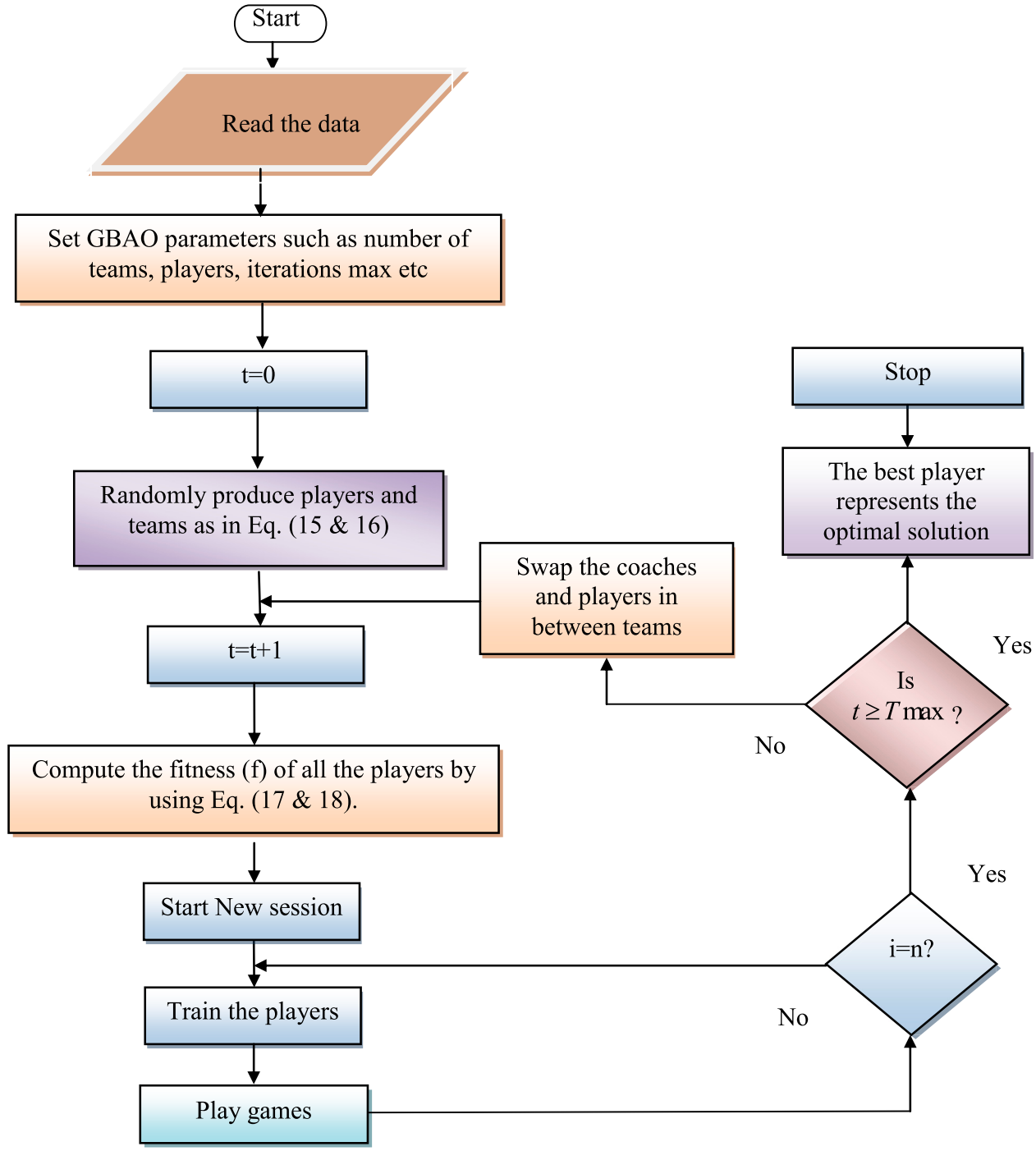

FIGURE 8
Flow chart of GBOA.

TABLE 3 System with SHAPF parameters.

Grid supply	V_s: 415Volts; f: 50Hertz R_s: 0.1Ω; L_s: 0.15 mH
SHAPF	R_{sh}: 0.0010 Ω; L_{sh}: 2.15 mH
DClink	C_{dc}: 9,400 microfarad; V_{dc}^{ref} = 700Volts

TABLE 4 Cases studies under 250 c solar Temperature.

	Case study 1	Case study 2	Case study 3	Case study 4
Grid Connected	✓	✓	✓	
Standalone				✓
Fixed solar irradiation (1000 W/m2)	✓			✓
Fixed solar irradiation (800 W/m2)		✓		
Variable solar irradiation			✓	
Load-1: Balanced bridged rectifier non-linear load: 60Ω and 30 mH	✓		✓	✓
Load 2: Unbalanced RL branch Load R1 = 10 Ω, R2 = 40 Ω and R3 = 80Ω L1 = 1.5mH, L2 = 3.5 mH and L3 = 2.5 mH		✓	✓	
Load 3: BLDC Motor drive	✓	✓	✓	✓
Load 4: Asynchronous Motor	✓			
Load 5: Active and Reactive power load p = 2000 W, 5000Vars		✓	✓	
THD	✓	✓	✓	
Power Factor	✓	✓	✓	
DC link voltage settling time (sec)	✓	✓	✓	✓

TABLE 5 Comparison of %THD.

Ref []/Controller	Case-1	Case-2	Case-3
Without SHAPF	28.99	11.36	27.33
PIC	6.01	5.12	6.12
FLC	4.48	3.99	4.89
SMC	4.91	3.54	4.97
GBOA-FLC	2.27	2.24	4.55

supply reduce converter ratings and stress by alleviating the demands imposed by the utility. Eq. 7 yields the recommended technique's PL.

$$P_{PV} \pm P_{BSS} + P_G = P_L \tag{7}$$

2.2.1 SES

The PV version employed in this investigation was selected from the Simulink library. However, to achieve the necessary voltage and current, the PV modules are connected in a series arrangement to form a string. Consequently, several of the above strings are joined together in parallel. Every PV cell within the module is constructed with a simpler circuit comprising just one diode, as depicted in Figure 2.

The PV cell's output current is determined by applying Kirchhoff's law as stated in Eq. 8

$$i_{PV} = i_{ph} - i_d - i_{sh,PV} \tag{8}$$

Eq. 9 links the PV modules in both series and parallel configurations, forming an array and Eq. 10 gives the PV current.

$$i_{PV,m} = i_{ph}N_p - i_{S,PV}N_p\left[\exp\left(\frac{Q\left(V_{PV} + N_s/N_p\left(i_{PV,m}R_{S,PV}\right)\right)}{N_s\eta kT_C}\right) - 1\right] - \frac{V_{PV,m} + N_s/N_p\left(i_{PV,m}R_{S,PV}\right)}{N_s/N_p\left(R_{sh,PV}\right)} \tag{9}$$

Here,

$$i_{ph} = \left(i_{ph,n} + K_1\Delta T_C\right)\frac{G}{G_n} \tag{10}$$

Here, "PPV, VPV, iPV" resembles solar output power, voltage and current. "iph, id, ish,PV" gives photo current, diode current and shunt PV current. "Np, Ns, T, G" indicates number of cells in parallel, series, temperature and irradiation. Suffix "m" indicates module.

Eq. 11 describes the solar output whose controller is given in the Figure 3. The FLC-basedMPPT method (Discussed in Section 3 in detail) was adopted in this work to extract maximum output.

$$P_{PV} = V_{PV} \times i_{PV} \tag{11}$$

2.2.2 ESS

The lithium-ion ESS offers advantages such as low self-discharge and minimal maintenance requirements. The battery can undergo charging or discharging processes utilizing switches SW1 and SW2, as depicted in Figure 4A. Eq. 12 represents the state-of-charge (SOCB) of the battery.

$$SOCB = 80\left(1 + \int i_{BS}\,dtQ\right) \tag{12}$$

The battery's ability to charge or discharge depends upon the quantity of SES and SOCB limits.

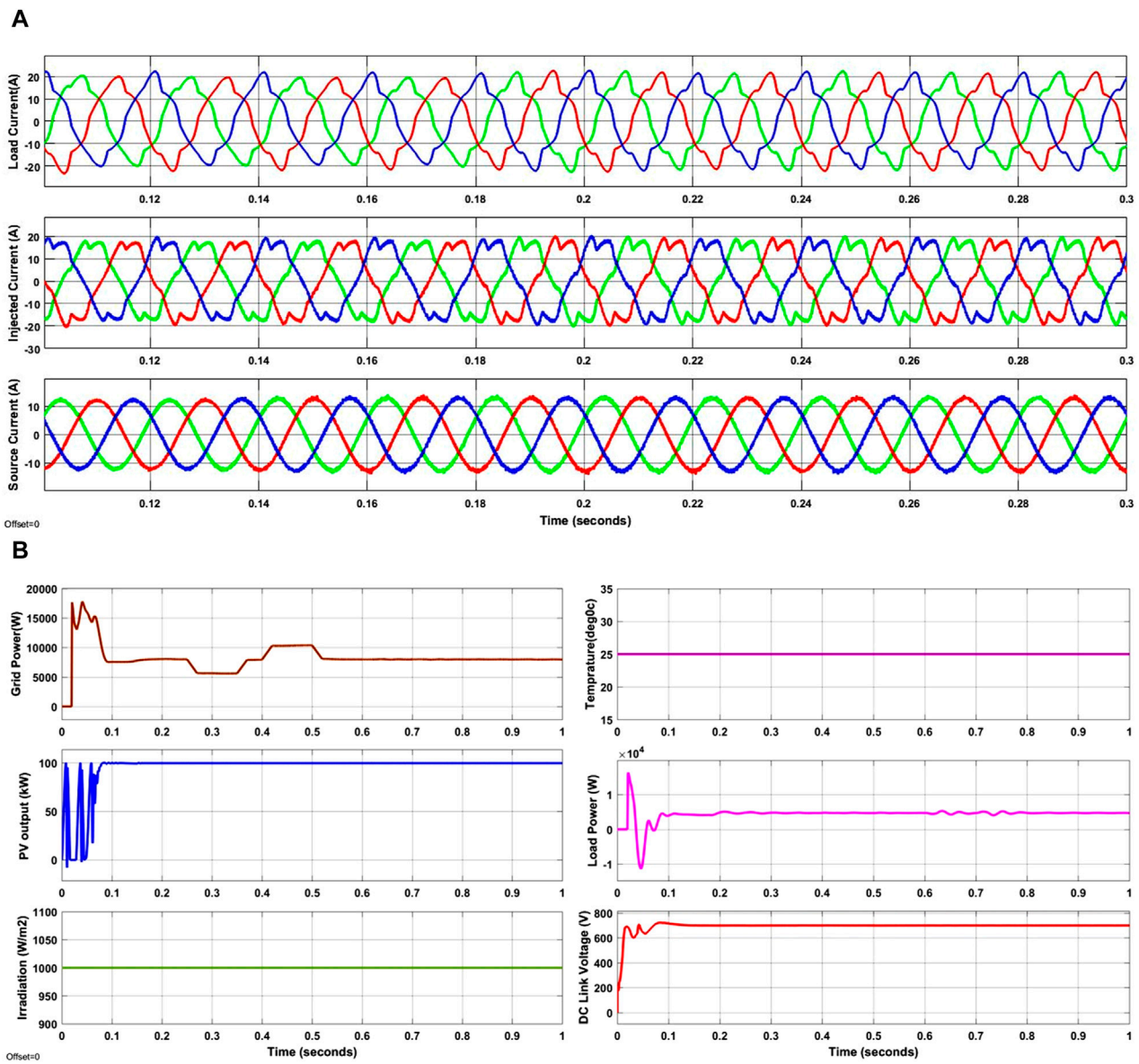

FIGURE 9
Waveforms of the suggested method for case one. **(A)** i_l, i_{sh}, i_s **(B)** Grid power, P_{PV}, G, T, P_L, DCLCV.

$$SOCB_{\min} \le SOCB \le SOCB_{\max} \quad (13)$$

In this Eq. 13, the symbol "SOCB" represents the battery's state of charge and current. "SOCBmax" and "SOCBmin" show the maximum and minimum permissible values for the state of charge of the battery. Figure 4B depicts the control circuit regulating the battery operation concerning the desired DCLCV. Table 1 presents the power management of SES and ESS in conjunction with the grid and load. Table 2 displays the selected SES and ESS values for the project.

3 Control scheme

The primary objectives of SHAF are to maintain the DCLCV at a consistent level and mitigate waveform abnormalities by providing an optimal current. It does the following frame conversions: (i) abc to dq0 and *vice versa* (ii) GBOA-based Fuzzy is developed to fulfill the specific objectives. As the published works already contain conversions, this paper focuses on highlighting the control approach of the proposed GBOA-based Fuzzy.

3.1 FLC

The FLC is advised to keep the DLCV steady. The reference voltage is compared to the actual voltage for DLCV stabilization, and its error is expressed as Error (E), Change in Error (CE), and Output (O), with Two Input Single Output (TISO). The following are regarded as inputs and outputs: Negative-Big (NGTB), Negative

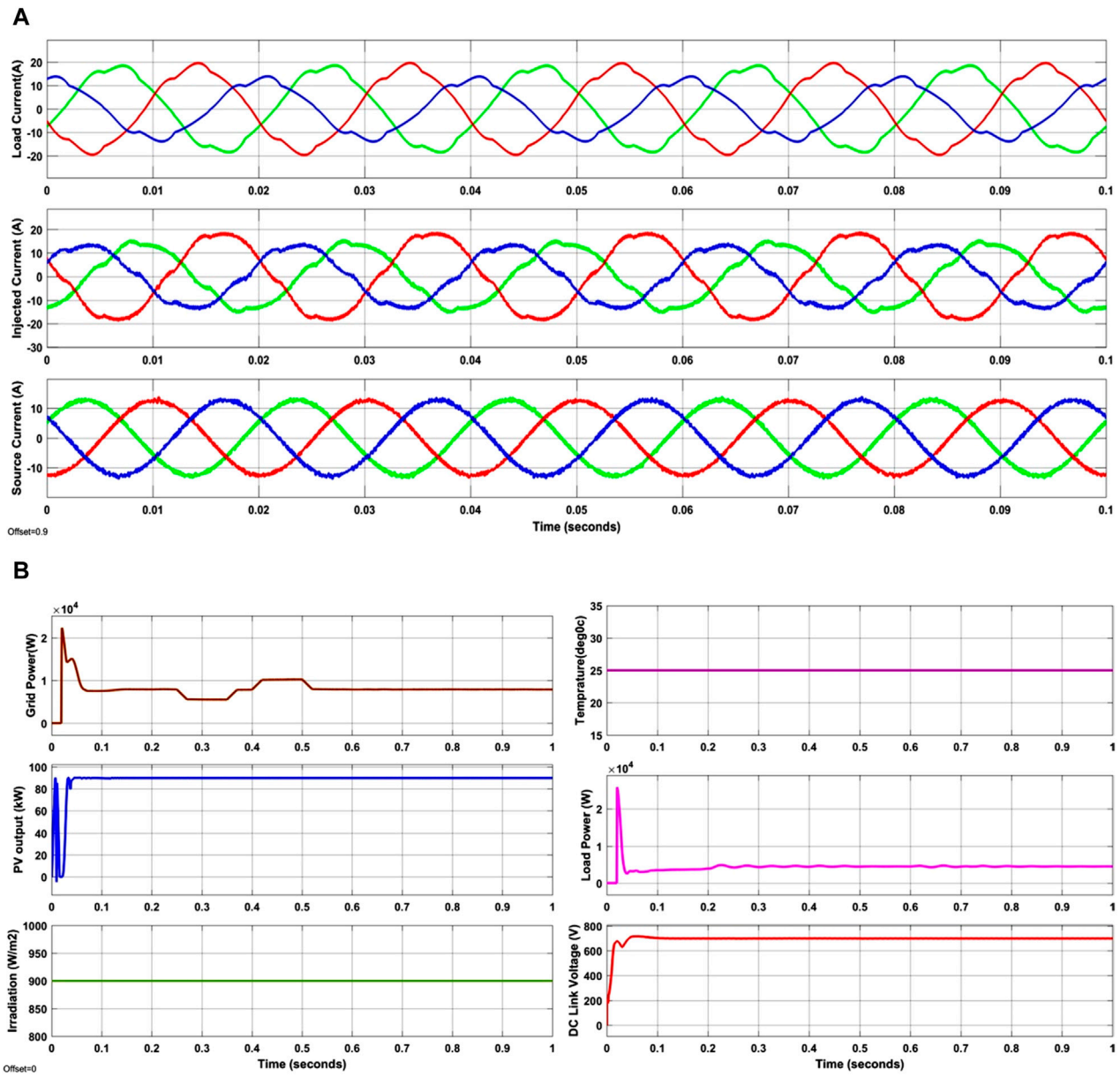

FIGURE 10
Waveforms of the suggested system for case two. **(A)** i_l, i_{sh}, i_s **(B)** Grid power, P_{PV}, G, T, P_L, DCLCV.

medium (NGTM), Zero (ZERO), Positive small (POSS), Positive big (POSB), Positive medium (POSM), and Negative-small (NGTS).

Here, the GBOAis adopted to optimize MSF parameters, the problem was set up for a triangular MSF (The same argument can be extended to two input MSF and output in the present work) as follows: Define the span given by Eq. (14). of the MSF using ai, bi and ci as in Figure 5.

$$triangle(x;a,b,c) = \begin{cases} 0 & x_{\min} \le a \\ \dfrac{x-a}{b-a} & a \le x \le b \\ \dfrac{c-x}{c-b} & b \le x \le c \\ 0 & c \le x_{\max} \end{cases} \quad (14)$$

Where, the range (Universe of discourse) of x is xmax - xmin (upper and lower bonds) which are considered as 1 and -1 (normalized) and i is the fuzzy set. The task is to improve the performance of the FLC by optimizing the MSF parameters.

3.2 GBOA based MSF selection

The GBOA method is a meta-heuristic that utilizes several populations. Like other population-based methodologies, GB initiates its execution by generating a population of solutions. Subsequently, it allocates the various problem-solving approaches into distinct teams, each operating autonomously and engaging in a competitive confrontation.

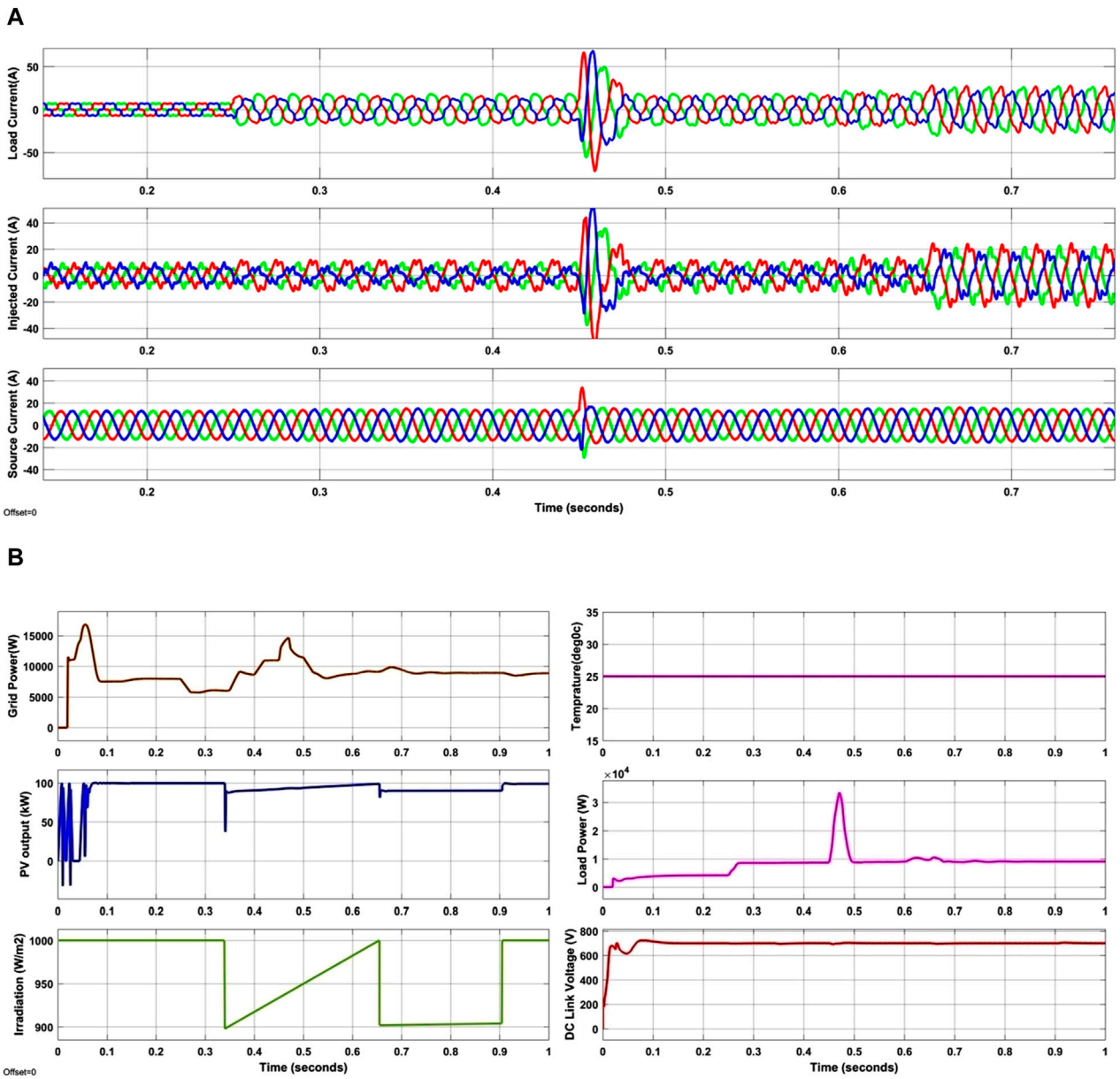

FIGURE 11
Waveforms of the suggested system for case three. **(A)** i_l, i_{sh}, i_s **(B)** Grid power, P_{PV}, G, T, P_L, DCLCV.

This competition is crucial in determining the transfer of solutions among teams and establishing the training model for each team.

The MSF control valuables a, b, c are arranged in the form of a matrix [f] of size (N × L), are K-number of parameters [u1,u2, ···,uK]. GBOA was developed from the inspiration of soccer games, where players in different teams attempt to play well to score goals and become the captain, in addition to winning the trophy. In this approach, a population of players are randomly generated and grouped into several teams. Each player in any team possessing different skills represents a solution of the clustering problem as,

$$Pij = \left[x_{ij}^{1}, x_{ij}^{2}, ..., x_{i}^{nv} j\right] \rightarrow [u_1, u_2....u_K] \\ = [(u_{11}, u_{12}....u_{1L}), (u_{11}, u_{12}....u_{1L})....., (u_{K1}, u_{K2}....u_{KL}) \quad (15)$$

Here in Eq. 15, uk denotes the k-th parameter, Pijis the j-th artificial player of the i-th team, and ukj is the j-th value of the k-th parameter. m and n represent the number of teams and the number of players in team, i. e., MSF variables that need to be optimized, respectively. Each player's contribution to a team is based on their abilities, which are assessed using a fitness function. The players with their teams comprise the population represented by Eq. 16,

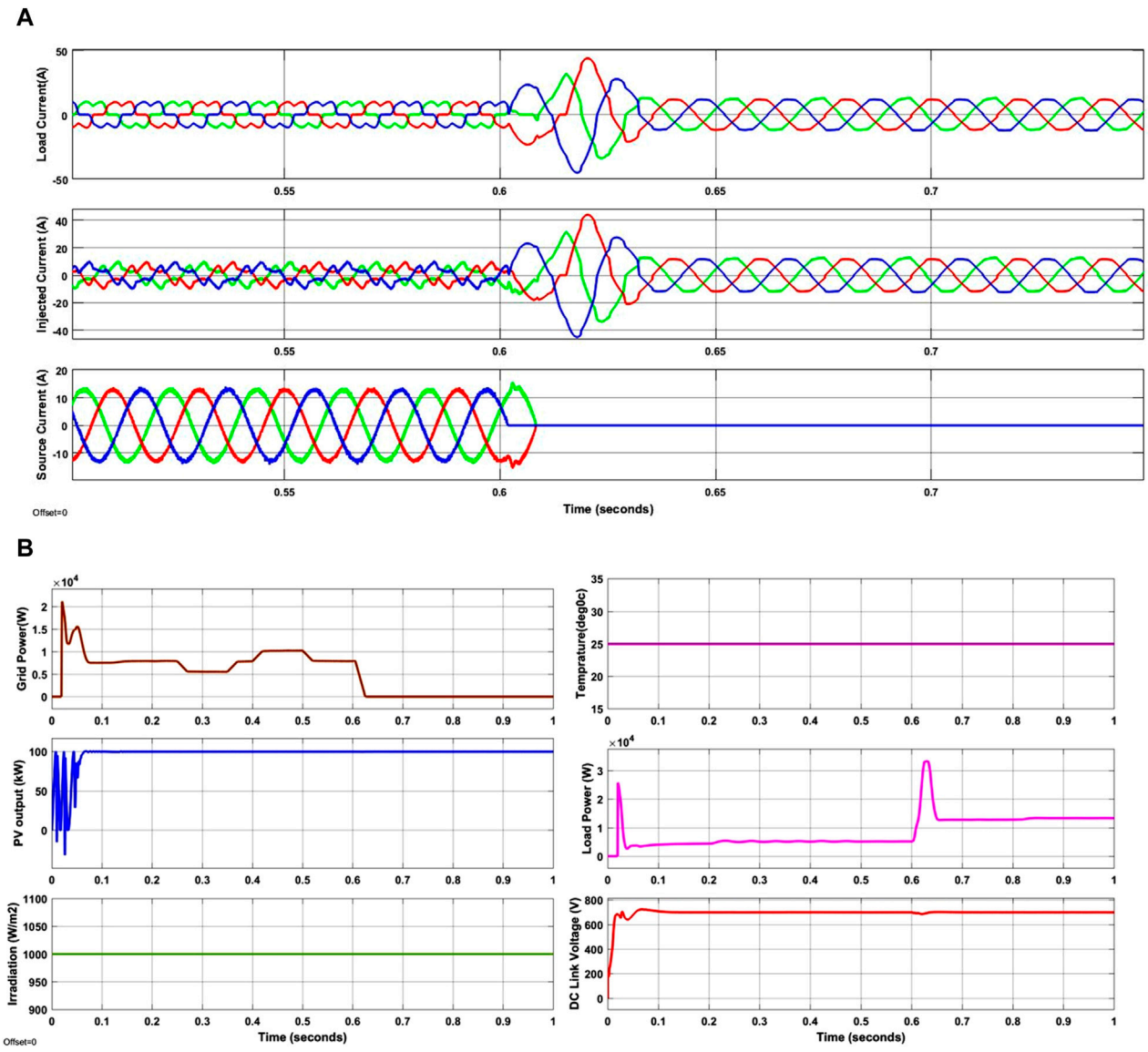

FIGURE 12
Waveforms of the suggested system for case four. **(A)** i_l, i_{sh}, i_s **(B)** Grid power, P_{PV}, G, T, P_L, DCLCV.

$$Population = \begin{bmatrix} T_1 \rightarrow \begin{Bmatrix} P_{11} \\ P_{12} \\ . \\ P_{1n} \end{Bmatrix} \\ T_2 \rightarrow \begin{Bmatrix} P_{21} \\ P_{22} \\ . \\ P_{2n} \end{Bmatrix} \\ . \\ . \\ T_m \rightarrow \begin{Bmatrix} P_{m1} \\ P_{m2} \\ . \\ P_{mn} \end{Bmatrix} \end{bmatrix} \tag{16}$$

Thus, the fitness function is customized using the minimization function of the issue as mentioned in Eq. 17,

$$Fitness\,function = \frac{1}{1 + MSE} \tag{17}$$

Where, is the actual output, indicated is the predicted output, and n is the total number of instances. The mean square error is then calculated using Eq. 18. where, O is the actual ouput, $\bar{O}$ indicated the predicted one, and n is the total number of instances.

$$MSE = \frac{1}{n}\sum_{p=1}^{m}\left(O_p - \bar{O}_p\right)^2 \tag{18}$$

The process describes to solve the MSF optimization. The global best solution are those that rank highest after optimization. Figure 6 shows the GBOA-based fuzzy optimal MSF. GBOA begins by generating the initial population and distributing the players, or solutions, among the system's subpopulations, or teams. After this preliminary stage is finished, the first season starts. Weeks make up a

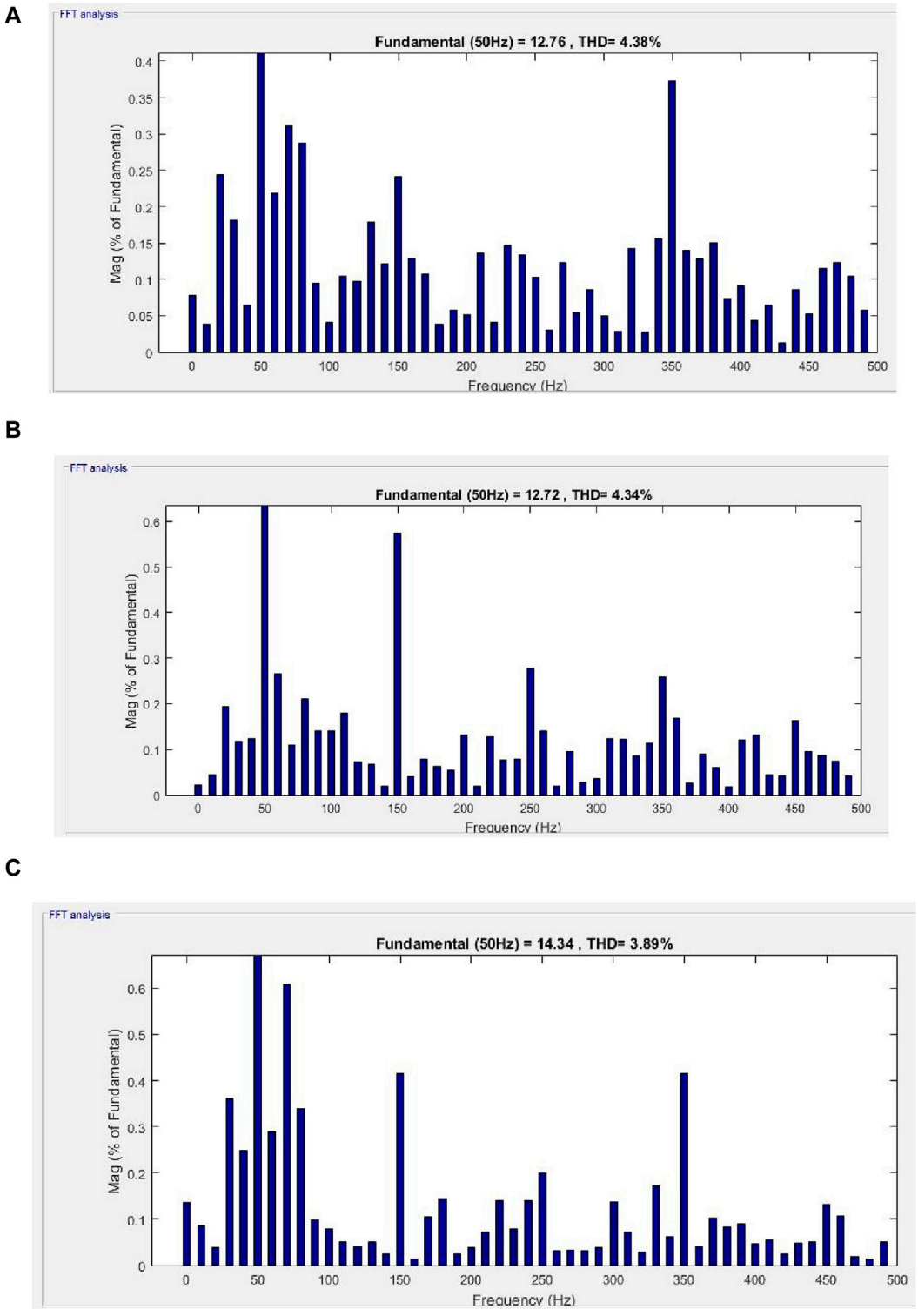

FIGURE 13
FFT spectrum for grid connected source current of three cases. **(A)** Case-1 **(B)** Case-2 **(C)** Case-3.

season, during which the teams practice and play one another to create a league competition. Following the season, there is a transfer window during which coaches and players can join new teams. Until the termination requirement is satisfied, this process is repeated. This work selected 4 teams and 12 players in each team and 10 times training of maximum 100 iterations (Tmax).

The load current is converted to the dq0 frame using the pharos approach, while the grid voltage sets the phasor through PLL. The

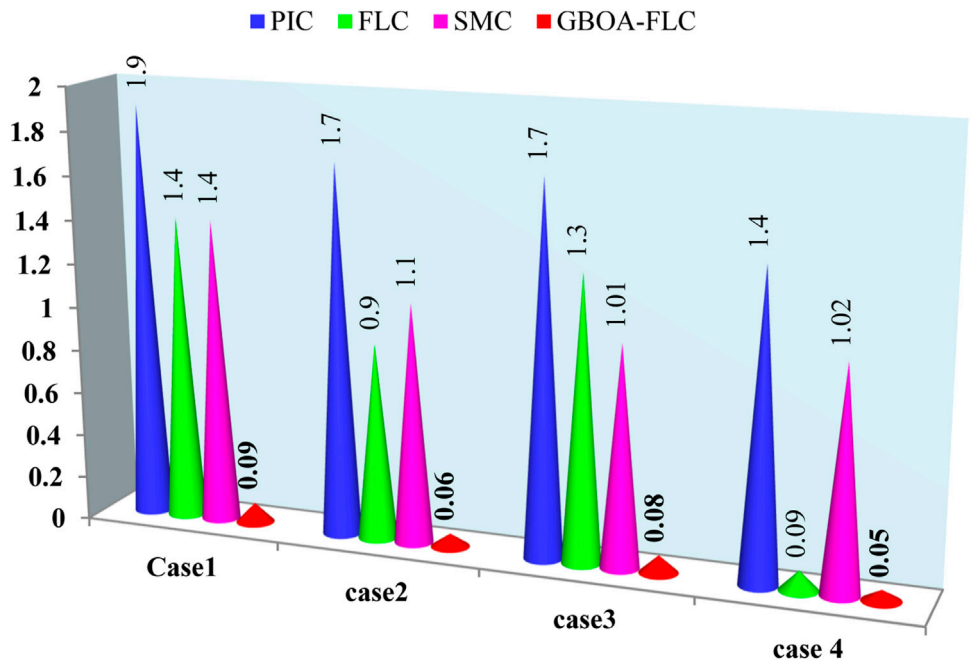

FIGURE 14
Comparison plot of time taken in sec to reach DCLCV stable.

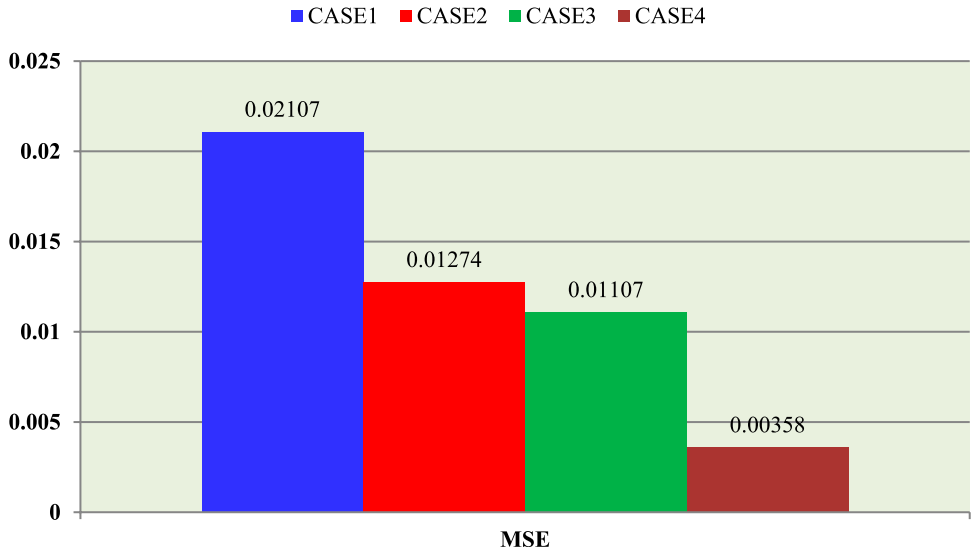

FIGURE 15
MSE for case studies.

performance of the SHAPF relies on the production of the reference current and the control of the DCLCV. However, as the load varies, it can lead to fluctuations in power flow, which in turn causes variations in DCLCV. To achieve stability in the DCLCV, the SHAPF must match the switching losses. The dth fraction of the load current is merged with the error obtained from the FLC. The dq0 components are converted into the abc reference frame and subsequently compared with the current at the load, and a hysteresis current controller is adapted to provide the necessary gate signals. Figure 7 depicts the regulation of SHAPF using the recommended controller. Figure 8 illustrates the flowchart of the suggested GBOA optimization technique.

4 Simulation and results

The given approach was tested using a 3-phase distribution system. Table 3 presents a record of the various parameters of the

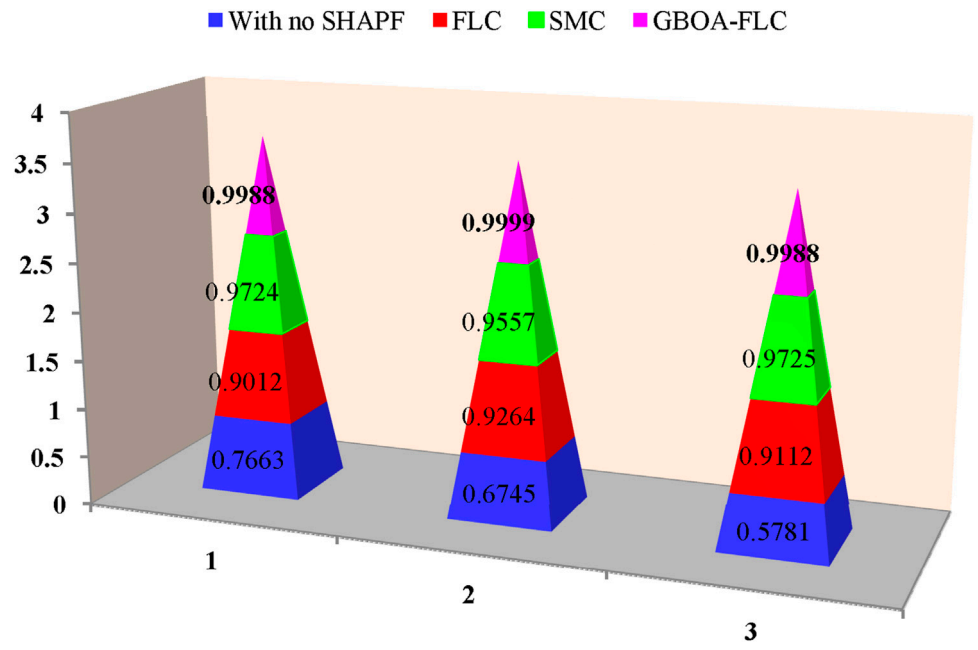

FIGURE 16
Power factor comparison.

system's configuration. To evaluate the effectiveness of the GBOA selected MSF of FLC-based SHAPF, four different test situations were chosen for grid/standalone conditions. These cases involved various combinations of harmonic loads, such as a three-phase rectifier load, an imbalanced load, an asynchronous motor load, an active/reactive power load, and BLDC Motor drive with fixed and variable SES. The details of these case studies may be seen in Table 4. The THD of the entire system were measured and compared with the commonly used SMC and FLC methods in Table 5 for each test scenario, both with and without the usage of SHAPF.

The suggested system's waveforms for cases 1–4 are shown in Figures 9–12. These represent the load voltage (Vl), DCLCV (Vdc) voltages, irradiation (G), and temperature (T).

Table 4 demonstrates that in case 1, when Load1, Load 3 and Load 4 are connected, the current in the load is not sinusoidal. However, it is balanced with a power factor of 0.7663 and a THD of 28.99%. Figure 9A shows that the proposed system offers a distortion-free supply current. In addition to the existing waveforms, there is a notable decrease in the THD, as indicated in Table 5. By introducing the suitable shunt currents, the power factor increased from 0.7663 to 0.9988 and the THD of the load current dropped from 28.99% to 2.27%—a lower value compared to other methods and documented techniques. As depicted in Figure 9B, the proposed method successfully achieved a stable DCLCV within a time frame of less than 0.09 s. However, it is also clearly visible that during supply changes the solar under fixed G of 1000 W/m2 and 250c temperature conditions is satisfying load demand effectively.

As seen in Figure 10A, the load current in case 2 was extremely imbalanced and non-sinusoidal due to the loads. As depicted in Figure 10A, the current waveform at load in case 2 exhibited a significant imbalance with non-sinusoidal pattern. The PF of the load current is observed to be 0.6745, whereas THD is 11.36% without a compensating device. Figure 10A demonstrates the ability of the designed system to generate sinusoidal grid current by eliminating harmonics and injecting the necessary amount of shunt compensating current. The PF is increased to almost 1 and the THD of the load current decreased from 11.36% to 2.24%. Moreover, it is clear that the proposed method settles the DCLCV at a consistent level of 0.06 s, during the change in grid supply; the Solar System provides the required power to satisfy the load demand as shown in Figure 10B.

Besides, case-3 demonstrates the dynamic behaviour a similar trend in reducing the THD and increasing the PF. The load current is initially non-sinusoidal and balanced till 0.25 s due to load 1. Later, at 0.25 s, load 2 is connected, due to which it exhibited non-synoidal and unbalanced. Lastly, at 0.45 s load 3 is connected, due to which the magnitude of current increases with imperfections. Lastly, at 0.65 s load 5 is connected. Figure 11A demonstrates that the proposed solution efficiently rectifies the shortcomings in the present waveform. Furthermore, Figure 11B indicates that the proposed technique effectively maintains the stability of DCLCV within a short span of 0.05 sec. Besides, it is visible that the demand is satisfied successfully during both the grid power and solar power variations.

The case 4 provides the study during grid and standalone conditions with loads 1 and 3 acting simultaneously. From Figure 12A, B it is clearly visible that the proposed system supplies distortion-free supply current till 0.6 s and successfully satisfies load demand with the grid's support. Later, from 0.6 s it works under the islanded mode of operation where the grid current is zero. However, it satisfies load demand with the support of the

Solar System. Additionally, it also reaches DCLCV stability with a very low time period of 0.05 s.

This study involves conducting FFT analysis on all test cases. However, this particular component focuses on the results of test case 3, which involved various types of non-linear and unbalanced loads in conjunction with a BLDC Motor drive. The current harmonic spectra are depicted for each scenario in Figure 13. Figure 14 displays the recorded time required for the stable-state DCLCV and various control systems. This shows that the BGOA-tuned PIC-based SHAPF achieves steady-state DCLCV in under 0.02 s. Figure 15 illustrates MSE for various case studies considered and the power factor comparison for all four cases is shown in Figure 16. The talks above demonstrate that the proposed technique is highly effective in reducing total THD, enhancing PF, and ensuring the stability of the DCLCV.

5 Conclusion

In this paper, the reduced switch shunt VSC was created for the SHAPF. The GBOA was developed to optimize the selection of MSF and FLC for the proposed shunt converters. The ESS controller and different SHAPF, solar, and ESS components were also included in the modeling process. This facilitated prompt intervention in adjusting the DCLCV, reducing the THD of source currents, and enhancing the power factor. By analyzing three test scenarios with varying load topologies, fixed and variable G, the proposed controller effectively reduces THD to levels that fall within acceptable limits and significantly improves the power factor to close to unity. These controllers performed better than the commonly employed FLC and SMC controllers. In addition, the suggested system demonstrated a faster stable DCLCV attainment than alternative techniques. Subsequent research on the proposed model could focus on enhancing the design parameters of the model by approaching the design challenge as optimization problem and employing metaheuristic optimization techniques.

Data availability statement

The original contributions presented in the study are included in the article/supplementary material, further inquiries can be directed to the corresponding author.

Author contributions

KS: Conceptualization, Methodology, Writing–original draft. DS: Software, Writing–review and editing. SG: Conceptualization, Methodology, Writing–original draft. RV: Data curation, Investigation, Writing–original draft. PB: Supervision, Writing–review and editing. IC: Supervision, Writing–review and editing. SS: Funding acquisition, Writing–review and editing.

Funding

The author(s) declare that no financial support was received for the research, authorship, and/or publication of this article.

Conflict of interest

The authors declare that the research was conducted in the absence of any commercial or financial relationships that could be construed as a potential conflict of interest.

Publisher's note

References

Abdelnasser, A., Nafeh, A. H., El-SehiemyRagab, A., and Waleed, A. A. S. (2022). Intelligent fuzzy-based controllers for voltage stability enhancement of AC-DC micro-grid with D-STATCOM. *Alexandria Eng. J.* 61, 2260–2293. doi:10.1016/j.aej.2021.07.012

AlapatiRamadevi, K. S., Praveen Kumar Balachandran, I. C., Dhanamjayulu, C., Khan, B., and Khan, B. (2023). Optimal design and performance investigation of artificial neural network controller for solar- and battery-connected unified power quality conditioner. *Int. J. Energy Res.* 2023, 1–22. Article ID 3355124. doi:10.1155/2023/3355124

AlifMansor, M., Hasan, K., Murtadha Othman, M., Noor, S. Z. B. M., and Musirin, I. (2020). Construction and performance investigation of three-phase solar PV and battery energy storage system integrated UPQC. *IEEE Access* 8, 103511–103538. 2997056. doi:10.1109/access.2020.2997056

Chandrasekaran, K., Selvaraj, J., Amaladoss, C. R., and Veerapan, L. (2021). Hybrid renewable energy based smart grid system for reactive power management and voltage profile enhancement using artificial neural network. *Energy Sources, Part A Recovery, Util. Environ. Eff.* 43 (No. 19), 2419–2442. doi:10.1080/15567036.2021.1902430

Das, S. R., Ray, P. K., Mohanty, A., and Panda, G. (2021). "Power quality enhancement in PV and battery storage based microgrid using hybrid active filter," in 2020 3rd International Conference on Energy, Power and Environment: Towards Clean Energy Technologies, China, 5th-7th March, 2021 (IEEE), 5–7.

Devassy, S., and Singh, B. (2020). Performance analysis of solar PV array and battery-integrated unified power quality conditioner for micro grid systems. *IEEE Trans. Industrial Electron.* 5 (Issue), 4027–4035. doi:10.1109/TIE.2020.2984439

Dheeban, S. S., and MuthuSelvan, N. B. (2021). ANFIS-based power quality improvement by photovoltaic integrated UPQC at the distribution system. *IETE J. Res.*, 1–19. doi:10.1080/03772063.2021.1888325

Jaber, S., and Shakir, A. M. (2021a). Design and simulation of a boost-microinverter for optimized photovoltaic system performance. *Int. J. Smart Grid* 5 (No. 2), 1–9. doi:10.20508/ijsmartgrid.v5i2.189.g145

K Krishna, V., Dash, S. K., and Geshma, K. (2020nd). "Development and analysis of power quality by using fuel cell based shunt active power filter," in International Conference on Innovative Mechanisms for Industry Applications (ICIMIA), 5-7 March 2020, USA, 5-7 March, 2020 (IEEE).

Kumar, N., Singh, B., and BijayaKetanPanigrahi, (2019). Grid synchronisation framework for partially shaded solar PV-based microgrid using intelligent control strategy. *Transm. Distribution* 13 (No 6), 829–837. doi:10.1049/iet-gtd.2018.6079

Kumar, N., Singh, B., and Panigrahi, B. K. (2023). Voltage sensorless based model predictive control with battery management system: for solar PV powered on-board EV charging. *IEEE Trans. Transp. Electrification* 9 (2), 2583–2592. doi:10.1109/TTE.2022.3213253

Kumar, N., Singh, B., Wang, J., and Panigrahi, B. K. (2020). A framework of L-HC and AM-MKF for accurate harmonic supportive control schemes. *IEEE Trans. Circuits Syst. I Regul. Pap.* 67 (12), 5246–5256. doi:10.1109/TCSI.2020.2996775

Kumari, P., Kumar, N., and Panigrahi, B. K. (2023). A framework of reduced sensor rooftop SPV system using parabolic curve fitting MPPT technology for household consumers. *IEEE Trans. Consumer Electron.* 69 (1), 29–37. doi:10.1109/TCE.2022.3209974

Mohanraj, M. R., and Prakash, R. (2020). A unified power quality conditioner for power quality improvement in distributed generation network using adaptive distributed power balanced control (ADPBC). *Int. J. Wavelets, Multi-resolution Inf. Process.* 18 (No. 01), 1941021. doi:10.1142/s0219691319410212

Nagireddy, V. V., Kota, V. R., and Ashok Kumar, D. V. (2018). Hybrid fuzzy back-propagation control scheme for multilevel unified power quality conditioner. *Ain Shams Eng. J.* 9 (4), 2709–2724. doi:10.1016/j.asej.2017.09.004

Nkado, F., Nkado, F., Oladeji, I., and Zamora, R. (2021). Optimal design and performance analysis of solar PV integrated UPQC for distribution network, EJECE. *Eur. J. Electr. Eng. Comput. Sci.* 5 (5), 1–8. doi:10.24018/ejece.2021.5.5.361

Pazhanimuthu, C., and Ramesh, S. (2018). Grid integration of renewable energy sources (RES) for power quality improvement using adaptive fuzzy logic controller-based series hybrid active power filter (SHAPF). *J. Intelligent Fuzzy Syst.* 35 (No. 1), 749–766. doi:10.3233/jifs-171236

Rajesh, P., Shajin, F. H., and Umasankar, L. (2021). A novel control scheme for PV/wt/FC/battery to power quality enhancement in micro grid system: a hybrid technique. *Util. Environ. Eff.*, 1–17. doi:10.1080/15567036.2021.1943068

Ray, P., Ray, P. K., and Dash, S. K. (2022). Power quality enhancement and power flow analysis of a PV integrated UPQC system in a distribution network. *IEEE Trans. onIndustry Appl.* 1 (58), 201–211. doi:10.1109/TIA.2021.3131404

Renduchintala, U. K., Pang, C., Tatikonda, K. M., and Yang, L. (2021). ANFIS-fuzzy logic based UPQC in interconnected microgrid distribution systems: modeling, simulation and implementation. *J. Eng.* 21 (No.1), 6–18. doi:10.1049/tje2.12005

SaiSarita, N. C., Suresh Reddy, S., and Sujatha, P., "Control strategies for power quality enrichment in Distribution network using UPQC", 2021.

Sarker, K., Chatterjee, D., and Goswami, S. K. (2020). A modified PV-wind-PEMFCS-based hybrid UPQC system with combined DVR/STATCOM operation by harmonic compensation. *Int. J. Model. Simul. World Sci.* 41 (No.4), 243–255. doi:10.1080/02286203.2020.1727134

Saxena, V., Kumar, N., Singh, B., and Panigrahi, B. K. (2021). An MPC based algorithm for a multipurpose grid integrated solar PV system with enhanced power quality and PCC voltage assist. *IEEE Trans. Energy Convers.* 36 (2), 1469–1478. doi:10.1109/TEC.2021.3059754

Sayed, J. A., Sabha, R. A., and Ranjan, K. J. (2021). Biogeography based optimization strategy for UPQC PI tuning on full order adaptive observer-based control. *IET Generation, Transm. Distribution* 15, 279–293. doi:10.1049/gtd2.12020

Siu, J. Y., Kumar, N., and Panda, S. K. (2022). Command authentication using multiagent system for attacks on the economic dispatch problem. *IEEE Trans. Industry Appl.* 58 (4), 4381–4393. doi:10.1109/TIA.2022.3172240

Srilakshmi, K., Krishna Jyothi, K., Kalyani, G., and SaiPrakashGoud, Y. (2023). Design of UPQC with solar PV and battery storage systems for power quality improvement. *Cybern. Syst.*, 1–30. doi:10.1080/01969722.2023.2175144

Srilakshmi, K., Rao, G. S., Swarnasri, K., Inkollu, S. R., Kondreddi, K., Balachandran, P. K., et al. (2024). Optimization of ANFIS controller for solar/battery sources fed UPQC using an hybrid algorithm. *ElectrEng*. doi:10.1007/s00202-023-02185-8

Srilakshmi, K., Srinivas, N., Balachandran, P. K., Reddy, J. G. P., Gaddameedhi, S., Valluri, N., et al. (2022). Design of soccer league optimization based hybrid controller for solar-battery integrated UPQC. *IEEE Access* 10, 107116–107136. doi:10.1109/ACCESS.2022.3211504

SrilakshmiKoganti, G. S., Reddy, B. S., Praveen Kumar, B., Prasad, R. G., PalanivelуAravindhababu, S. S., et al. (2024). Optimal design of solar/wind/battery and EV fed UPQC for power quality and power flow management using enhanced most valuable player algorithm. *Front. Energy Res.* 11. doi:10.3389/fenrg.2023.1342085

Tawfiq, A. E., El-Raouf, M. O. A., Mosaad, M. I., Gawad, A. F. A., and Farahat, M. A. E. (2021). Optimal reliability study of grid-connected PV systems using evolutionary computing techniques. *IEEE Access* 9, 42125–42139. doi:10.1109/ACCESS.2021.3064906

Vinothkumar, V., and Kanimozhi, R. (2021). RETRACTED ARTICLE: power flow control and power quality analysis in power distribution system using UPQC based cascaded multi-level inverter with predictive phase dispersion modulation method. *J. Ambient Intell. Humaniz. Comput.* 12, 6445–6463. doi:10.1007/s12652-020-02253-y